Lithium Nitrate As Regenerable SEI Stabilizing Agent for Rechargeable Li/O2 Batteries

6 AUTHORS, INCLUDING:

Jasim Uddin

California Institute of Technology

44 PUBLICATIONS   **1,526** CITATIONS

SEE PROFILE

Vyacheslav S Bryantsev

Oak Ridge National Laboratory

78 PUBLICATIONS   **2,246** CITATIONS

SEE PROFILE

Vincent Giordani

Liox Power, Inc.

23 PUBLICATIONS   **617** CITATIONS

SEE PROFILE

Dan Addison

Independent Researcher

21 PUBLICATIONS   **301** CITATIONS

SEE PROFILE

Lithium Nitrate As Regenerable SEI Stabilizing Agent for Rechargeable Li/O₂ Batteries

Jasim Uddin,* Vyacheslav S. Bryantsev, Vincent Giordani, Wesley Walker, Gregory V. Chase, and Dan Addison*

Liox Power, Inc., 129 North Hill Avenue, Suite 103, Pasadena, California 91106, United States

Ⓢ Supporting Information

ABSTRACT: A major unsolved problem with rechargeable Li/O₂ batteries is the identification of electrolyte compositions that allow efficient and stable cycling of both Li metal and O₂ electrodes simultaneously. Previously, lithium nitrate (LiNO₃) was employed in a rechargeable Li/O₂ battery to stabilize the solid−electrolyte interphase on Li metal in an electrolyte based on *N,N*-dimethylacetamide (DMA), a solvent with favorable properties vis-à-vis the O₂ electrode. We show that LiNO₃ is regenerated following reaction with Li metal in the presence of dissolved O₂, which may account for the surprising long-term cycling previously demonstrated in DMA. According to this new concept, nitrate anions incorporated into the electrolyte react with Li metal to form soluble nitrite anions and a passivating layer of Li₂O on the Li electrode surface. The soluble nitrite anions subsequently react with dissolved O₂ through a combined electrochemical and chemical process that results in regeneration of nitrate. Discovery of this regenerative principle provides a strategy for using other solvents that have favorable characteristics in the O₂ electrode but are highly unstable toward Li metal without the use of a ceramic Li-ion-conducting membrane.

SECTION: Energy Conversion and Storage; Energy and Charge Transport
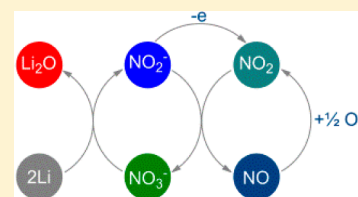
A s one of the few possible rechargeable battery systems having specific energy within an order of magnitude of gasoline, Li/O₂ batteries are a current target of research and development for electric vehicles.[1] Two frequently cited Li/O₂ cell designs involve (1) directly coupling a metallic Li electrode to an O₂ electrode through an organic liquid electrolyte and (2) interposing a solid, inorganic Li⁺-conducting membrane between a metallic Li electrode and an O₂ electrode containing an organic liquid electrolyte.[2] The overall reaction for both cell configurations is:

$$2Li + O_2 \rightarrow Li_2O_2 \qquad (1)$$

In principle, the second design decouples the operating environment of the two electrodes, allowing different electrolyte materials that are optimized for each respective electrode to be employed on either side of the membrane. Unfortunately, no Li⁺-conducting membrane materials have demonstrated adequate performance in contact with nonaqueous O₂ electrodes over multiple cycles. The paucity of known classes of effective solid Li⁺-conducting membrane materials motivates research in the first cell design, but major challenges are encountered in this system as well. Few organic liquid electrolytes enable Li metal electrode operation that is safe and efficient enough for commercial rechargeable battery applications.[3] The O₂ electrode further constrains electrolyte composition because many polar, aprotic solvents participate in parasitic reactions with O₂ reduction reaction (ORR) intermediates and products.[4−8] Still more vexing, the particular solvent classes that work comparatively well with metallic Li electrodes, namely, ethers and carbonates, undergo significant

decomposition in the O₂ electrode. To allow the direct pairing of an O₂ electrode with a metallic Li electrode through an organic liquid electrolyte, new approaches must be discovered to persistently stabilize the solid−electrolyte interphase (SEI) on Li metal in a wider range of solvent types.

Recently, Li/O₂ cells employing an electrolyte consisting of 1 M LiNO₃ in *N,N*-dimethylacetamide (DMA) were cycled for more than 2000 h while in situ electrochemical mass spectrometry measurements were performed periodically to monitor the composition of evolved gases during cell charging.[9] The results represent the longest calendar life Li/O₂ battery demonstrated to date having O₂ evolution and minimal (<5%) CO₂ evolution confirmed for each charging half cycle. DMA was selected as an electrolyte solvent because density-functional-theory-based calculations previously predicted and experiments confirmed the inertness of this solvent toward parasitic processes in the O₂ electrode.[10] Despite comparative stability in the O₂ electrode, DMA reacts vigorously with Li metal, resulting in the formation of dimethylamine gas, as determined via electrochemical mass spectrometry. No evidence of dimethylamine was observed in the presence of 1 M LiNO₃, suggesting that the SEI formed in this electrolyte inhibited the reaction between DMA and Li metal. In a subsequent study, symmetric Li/Li cells using the same electrolyte failed after ~120 h of stable, low polarization (~0.02 V) cycling under Ar gas but cycled with no failure yet
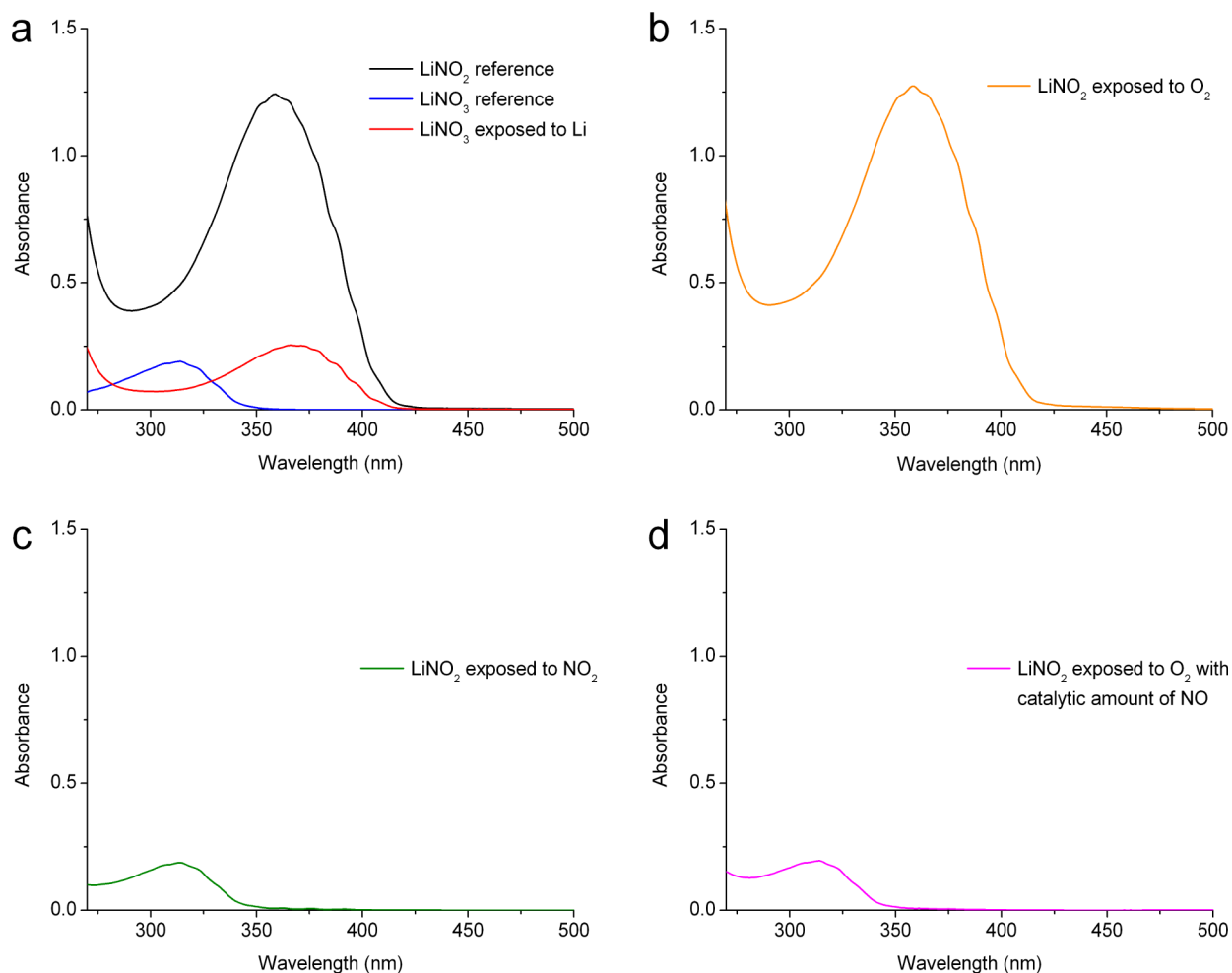
Figure 1. UV−visible absorption spectra including (a) $LiNO_2$ in DMA reference (black), $LiNO_3$ in DMA reference (blue), and a solution of 1 M $LiNO_3$ in DMA following exposure to Li metal with the $LiNO_3$ background spectrum subtracted (red). (b) $LiNO_2$ in DMA following exposure to 1 atm O_2 for 1 week. (c) $LiNO_2$ exposed to an equimolar amount of NO_2 and (d) $LiNO_2$ following exposure to O_2 in the presence of a catalytic amount of NO/NO_2.

observed (>4 months) under O_2 gas, demonstrating a surprising beneficial effect of O_2 in maintaining SEI stability in cooperation with $LiNO_3$.[11]

The use of electrolyte additives to stabilize the SEI on Li metal represents a promising approach toward improving Li metal electrode cycling characteristics in liquid electrolytes. In general, a drawback of this concept is that the irreversible consumption of the additive on Li metal may reduce the effect of the additive over time. For example, $LiNO_3$ is used in rechargeable Li/S batteries to prevent the reaction between the Li metal electrode and soluble polysulfides and is thought to react with Li metal according to the following reaction:[12]

$$2Li + LiNO_3 \rightarrow Li_2O + LiNO_2 \quad (2)$$

Insoluble Li_2O contributes toward an SEI that blocks the reduction of soluble polysulfides on Li metal, but SEI stability degrades over time as $LiNO_3$ is consumed.[13] In contrast, persistent inhibition of the reaction between DMA and Li metal in Li/O_2 cells employing $LiNO_3$ led us to conjecture that $LiNO_2$ formed in reaction 2 may be converted back to $LiNO_3$ in the presence of O_2. The present study provides rigorous experimental confirmation of a mechanism of regeneration of NO_3^- from NO_2^- that is uniquely possible in Li/O_2 cells. This regenerative mechanism may account for the surprisingly

prolonged cycling observed previously in Li/O_2 cells employing $LiNO_3$ in DMA and provides a new strategy to enable longer cycling using a wider range of solvent classes without the need for a ceramic membrane.
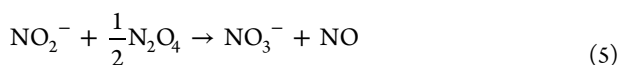
As a first step toward investigating the possible regeneration of NO_3^- from NO_2^- in rechargeable Li/O_2 cells, it was necessary to confirm the formation of $LiNO_2$ according to reaction 2. Very little literature exists on the synthesis and properties of $LiNO_2$, and the lack of reliable reference data on this species complicated the task of verifying its formation. In a previous study, electrochemical evidence of the presence of NO_2^- in the electrolyte of Li/O_2 cells containing $LiNO_3$ was obtained by the observation of a very small oxidative peak appearing in a linear sweep voltammogram (LSV) at ∼3.6 V versus Li/Li$^+$, which is approximately equal to the calculated thermodynamic potential for the oxidation of NO_2^-.[9]

To enable the present study, we proposed and validated a novel method of preparing $LiNO_2$, allowing the use of synthesized $LiNO_2$ to analyze its properties and reactivity. Ultraviolet−visible (UV−vis) spectroscopy was used throughout the investigation to confirm $LiNO_2$ formation and to understand the conversion between $LiNO_2$ and $LiNO_3$ under different experimental conditions. Initially, calibration curves for $LiNO_2$ and $LiNO_3$ dissolved in DMA were generated

(Figure S1 in the Supporting Information), and their molar extinction coefficients (ε) were calculated as 25.0 M^{-1} cm^{-1} and 3.7 M^{-1} cm^{-1}, respectively. The UV−vis reference spectra of 50 mM $LiNO_2$ and $LiNO_3$ in DMA were generated and compared with the spectrum of a sample electrolyte consisting of 1 M $LiNO_3$ in DMA exposed to a Li metal disk (Figure 1a). A peak at ~366 nm in both the $LiNO_2$ reference and the electrolyte sample exposed to Li metal confirms the formation of $LiNO_2$ in Li cells according to reaction 2. The solubility of both $LiNO_3$ and $LiNO_2$ were observed to be very high in DMA, with concentrations in excess of 5 M readily attainable.

Additionally, an experiment was performed to determine whether $LiNO_2$ reacts directly with O_2 in DMA. An electrolyte consisting of 1 M $LiNO_2$ in DMA was prepared and stored under 1 atm of O_2 gas for 1 week. The UV−vis spectrum observed after storage under O_2 reveals no evidence of the direct chemical oxidation of $LiNO_2$ to $LiNO_3$ (Figure 1b). Lack of direct reactivity between O_2 and NO_2^-, though thermodynamically favored, is expected based on observation of a high kinetic barrier for analogous reactions in systems of molten nitrates and nitrites with Na^+ and K^+ cations.[14]

The observation that NO_2^- is electrochemically oxidized within the charging potential range of the O_2 electrode in Li/O_2 cells led us to perform a mechanistic analysis of NO_2^- electrochemistry in DMA. A mechanism comprising electrochemical and chemical reactions has been previously conjectured to account for cyclic voltammetry (CV) data obtained in organic electrolytes under inert atmosphere comprising two successive oxidation waves:[15−17]

$$NO_2^- \rightarrow NO_2 + e \tag{3}$$

$$2NO_2 \rightleftharpoons N_2O_4 \tag{4}$$

$$NO_2^- + \frac{1}{2}N_2O_4 \rightarrow NO_3^- + NO \tag{5}$$

$$NO \rightarrow NO^+ + e \tag{6}$$

Combining steps 3−5, this mechanism predicts the formation of NO_3^- and NO gas during the first oxidation wave. Oxidation of NO gas generated in the first oxidation wave accounts for a second oxidation wave according to reaction 6. To evaluate this mechanistic framework in DMA, the 1D simulation program DigiElch 6.F was used to model the CVs of 6 mM $LiNO_2$ on a 5 mm diameter Pt macroelectrode at scan rates of 50, 100, and 200 mV/s. The only satisfactory fit with the experimental CV data was obtained when autoionization of N_2O_4 was explicitly incorporated into the model by substituting reactions 7 and 8 for reaction 5:

$$N_2O_4 \rightleftharpoons NO^+ + NO_3^- \tag{7}$$

$$NO_2^- + NO^+ \rightarrow NO_2 + NO \tag{8}$$

According to this mechanism, the first electron-transfer step (reaction 3) is followed by a series of rapid chemical reactions starting with dimerization of the resulting NO_2 (reaction 4), followed by autoionization of N_2O_4 (reaction 7) to form nitrosonium (NO^+) and NO_3^- ions and finally ionic recombination of NO_2^- with NO^+ (reaction 8). The reported equilibrium constants (log K) for the autoionization of N_2O_4 in nitromethane and sulpholane at 298 K are −9.2 and −7.2, respectively.[15] The strong solvating ability of DMA, a solvent with a comparatively high donor number, is expected to increase the ionic dissociation of N_2O_4 compared with

nitromethane and sulpholane. Furthermore, the ionic recombination of NO_2^- with NO^+ is expected to occur near the diffusion-controlled limit, which ultimately enables the conversion of NO_2^- into an equimolar mixture of NO_3^- and NO. Thus the sum of chemical steps (reactions 4, 7, and 8) and the overall electrochemical−chemical reaction corresponding to the first oxidation wave are stated in reactions 9 and 10, respectively:

$$NO_2 + NO_2^- \rightarrow NO_3^- + NO \tag{9}$$

$$2NO_2^- \rightarrow NO_3^- + NO + e \tag{10}$$
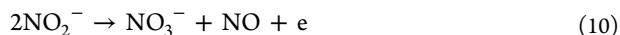
A fitting routine was used to establish the set of simulation parameters that provides the best average agreement between simulation and experiment at various scan rates (Table S1, Supporting Information). Figure 2 represents the best fit
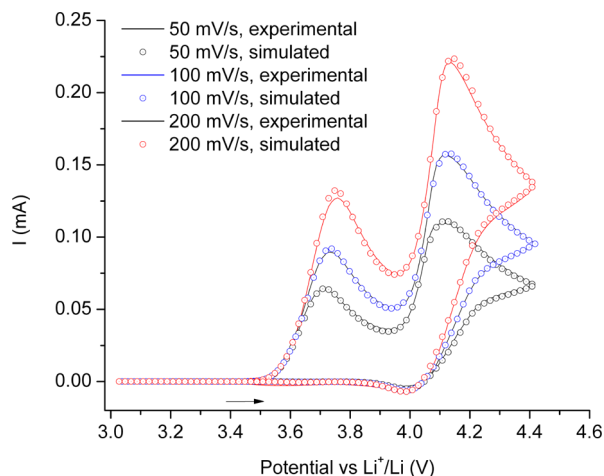

Figure 2. Comparison of experimental and simulated cyclic voltammograms for the oxidation of 6 mM $LiNO_2$ in 0.5 M LiTFSI/*N,N*-dimethylacetamide electrolyte on a Pt macroelectrode (d = 5 mm) at scan rates of 50, 100, and 200 mV/s. Cyclic voltammograms are shown after subtracting the background current and full IR compensation.

obtained from simulation. Using the simulation parameters listed in Table S1 (Supporting Information), it was possible to achieve adequate fits of CVs at all scan rates. We note that it was not possible to obtain a good fit to the experimental CVs by using reaction 9 directly, implying the validity of the proposed multistep mechanism in DMA solvent.

Direct evidence of the formation of NO_3^- and NO gas according to reactions 9 and 10 was obtained by UV−vis spectroscopy and mass spectrometry, respectively. First, equimolar amounts of $LiNO_2$ and NO_2 were combined in DMA in a reaction vessel, and a sample of the resulting solution was analyzed spectroscopically. The UV−vis absorption spectrum (Figure 1c) of the sample solution matches the reference spectrum for 50 mM of $LiNO_3$ (Figure 1a) and shows no absorption peak in the wavelength region of $LiNO_2$, demonstrating complete conversion of $LiNO_2$ to $LiNO_3$ via reaction 9.

Confirmation of NO formation according to reaction 10 was obtained by first performing LSV in a customized hermetically sealed electrochemical cell configured with an attached pressure sensor and a port allowing ex situ analysis of the head-space gas within the cell via mass spectrometry. The cell consisted of a Li metal counter electrode, a carbon paper working electrode, an
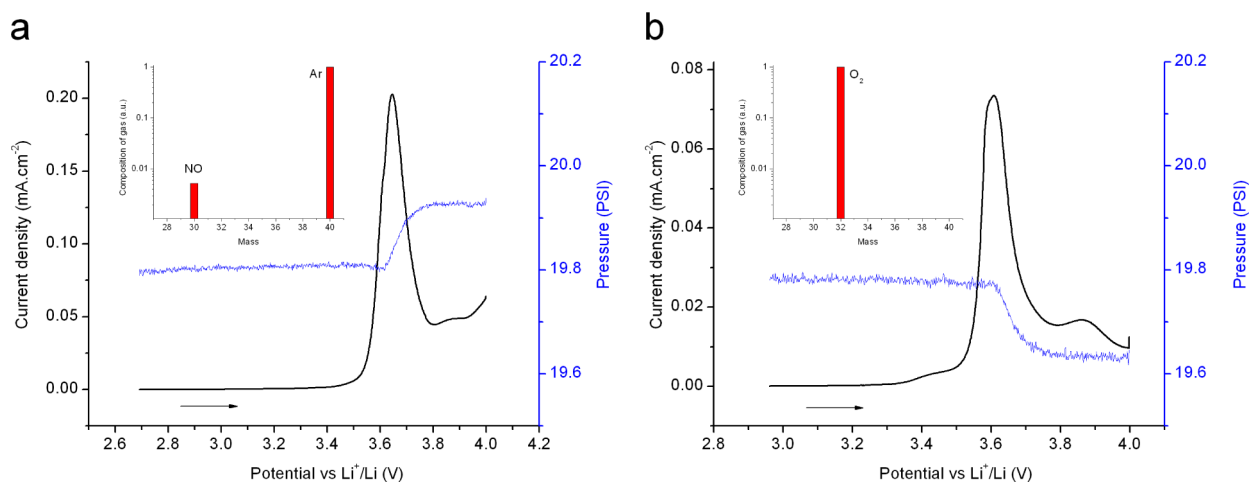
Figure 3. Linear sweep voltammograms with in situ pressure monitoring (blue curves) carried out in hermetically sealed fixtures, followed by analysis of the gas composition by mass spectrometry (insets) in cells containing (a) an Ar gas head space and (b) O_2 gas head space.

electrolyte consisting of 1 M $LiNO_3$ and 100 mM $LiNO_2$ in DMA under an Ar gas atmosphere. Results of the LSV experiment at a scan rate of 0.05 mV/s are depicted in Figure 3a. An oxidation wave corresponding to the initial one electron oxidation of NO_2^- is observed at the thermodynamically expected potential, which is accompanied by an increase in pressure corresponding to the evolution of gas into the head space of the hermetically sealed cell. Analysis of the head space gas via mass spectrometry confirmed the presence of NO (30 amu), the quantity of which is represented as a percentage of the Ar head space gas in the inset of Figure 3a. No other gases besides Ar and NO were detected within the mass range of the measurement.

The rapid reaction between NO and O_2 is involved in several established industrial processes (e.g., the Ostwald process):[18]

$$NO + \frac{1}{2}O_2 \rightarrow NO_2 \qquad (11)$$

We predicted on this basis that NO/NO_2 catalyzes the chemical oxidation of NO_2^- according to the sum of reactions 9 and 11:

$$NO_2^- + \frac{1}{2}O_2 \rightarrow NO_3^- \qquad (12)$$

According to this hypothesis, NO/NO_2 gases function as a chemical catalyst for the thermodynamically favored (−21 kcal/mol) though kinetically hindered reaction between NO_2^- and O_2 to form NO_3^- (reaction 12). To test this concept, we performed a second LSV experiment using the same fixture, cell configuration, and scan rate as in Figure 3a but substituting O_2 as the head space gas. In contrast with the experiment under Ar gas, a drop in pressure is observed synchronously with the first oxidation wave, and NO was not detected via mass spectrometry (Figure 3b, inset). The combination of a pressure drop, consistent with consumption of O_2, and absence of NO in the head-space gas provides clear evidence of the occurrence of reaction 12. Additionally, the peak current is considerably lower ($\sim$75 $\mu A/cm^2$) in the cell under O_2 compared with the cell under Ar ($\sim$200 $\mu A/cm^2$) despite the equal concentrations of NO_2^- in each experiment. This inequality is consistent with the hypothesized catalysis of reaction 12 by NO and the mechanistic framework for the electrochemical oxidation of NO_2^- previously described: As NO is generated (reaction 10),

it is quickly converted to NO_2 in the presence of O_2 (reaction 11), which reacts chemically with NO_2^- to form NO_3^- and more NO (reaction 9), the latter of which reenters this cycle by reacting again with O_2. Therefore, the consumption of NO_2^- by electrochemical oxidation competes with consumption by chemical oxidation under O_2, thus lessening available NO_2^- and thereby reducing peak current density.

To illustrate the effect of this catalytic principle, we carried out chemical reactions between O_2 and $LiNO_2$ in DMA in the same hermetically sealed cells. Figure 4 shows pressure versus
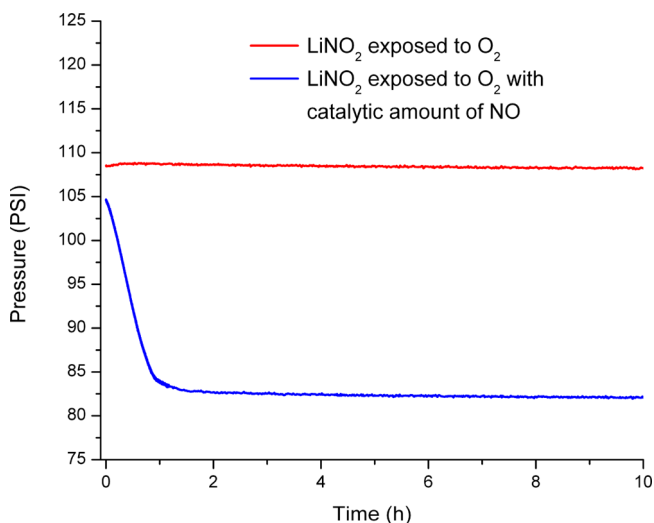

Figure 4. Pressure versus time curves of hermetically sealed reaction vessels containing $LiNO_2$ in DMA under pressurized O_2 gas both with a catalytic amount of NO/NO_2 (blue curve) and without NO/NO_2 (red curve).

time curves for cells containing pressurized O_2 gas and $LiNO_2$ dissolved in DMA with (blue curve) and without (red curve) a catalytic amount of NO/NO_2 (<1 psi). While no pressure drop is observed in the cell containing only O_2 gas and $LiNO_2$, a rapid pressure drop occurs in the cell containing a catalytic quantity of NO/NO_2, the magnitude of which corresponds to complete conversion of $LiNO_2$ to $LiNO_3$. This conversion is directly confirmed by UV−vis spectroscopy. The spectrum in Figure 1d, obtained from the sample plotted in blue in Figure 4,

matches the reference spectrum for $LiNO_3$, showing complete conversion of $LiNO_2$ in the presence of a catalytic amount of NO/NO_2.

The foregoing experiments provide clear empirical evidence for regeneration of NO_3^- from NO_2^- under conditions that exist in rechargeable Li/O_2 cells during the process of cell charging. As previously shown, consumption of NO_2^- occurs simultaneously through chemical (reaction 12) and electrochemical (reaction 3) pathways, such that the overall process can be summarized as follows:

$$nNO_2^- + (n-1)/2O_2 \rightarrow (n-1)NO_3^- + NO_2 + e \tag{13}$$
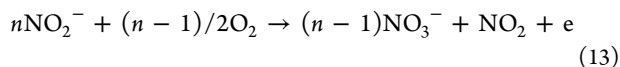
The value of n in this reaction depends on the relative rates of the electrochemical and chemical processes. Our data suggest a rapid chemical process relative to the electrochemical process, implying a large value for n, although reaction 13 predicts that at least a small quantity of NO_2 (or its corresponding dimer (reaction 4) or autoionized (reaction 7) forms) will be present at the end of charging.

We theorize that the regenerative mechanism demonstrated above accounts for the observed prolonged stability of the Li metal electrode previously observed in Li/O_2 cells containing $LiNO_3$. According to this theory, a stable SEI that substantially inhibits the reaction between Li metal and DMA is formed in the presence of $LiNO_3$ and maintained via the following steps:

(1) Li metal and $LiNO_3$ react according to: $2Li + LiNO_3 \rightarrow Li_2O + LiNO_2$ (reaction 2). The insoluble Li_2O provides a protective SEI on Li metal that allows passage of Li cations. While this SEI substantially inhibits further reaction with Li metal, reaction 2 continues, albeit at a slow rate, as Li metal changes volume and morphology during cycling, leading to a slow growth in the Li_2O film.

(2) Soluble $LiNO_2$ produced in reaction 2 freely diffuses to the positive electrode, where it is electrochemically oxidized on the first charging half cycle when the electrode potential exceeds 3.6 V. The product of this electrochemical oxidation is NO_2, which exists in equilibrium with its dimer and autoionized forms in polar aprotic solvents.

(3) Once a small amount of NO_2 is electrochemically generated following the first charging half cycle, a sequence of fast chemical reactions allows regeneration of $LiNO_3$ from $LiNO_2$ and dissolved O_2. These are: $LiNO_2 + NO_2 \rightarrow LiNO_3 + NO$ (reaction 9) and $NO + 1/2O_2 \rightarrow NO_2$ (reaction 11), the sum of which is $LiNO_2 + 1/2O_2 \rightarrow LiNO_3$ (reaction 12). Thus NO_2 (or its dimer and autoionized forms) serves to catalytically convert $LiNO_2$ to $LiNO_3$ in the presence of dissolved O_2 in the electrolyte.

To understand the fate of this remaining NO_2, we consider that the electrochemical reduction of NO_2 or its dimer and autoionized forms results in NO_3^- and NO according to the foregoing mechanism (reactions 3–9). The resulting NO reacts with O_2 according to reaction 11. Thus the overall reduction process is:

$$NO_2 + \frac{1}{2}O_2 + e \rightarrow NO_3^- \tag{14}$$
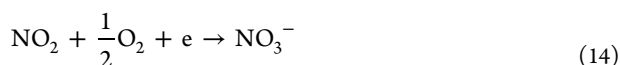
Consequently, all NO_2^- that is formed in the reaction between Li metal and NO_3^- (reaction 2) may be regenerated to NO_3^- in a cycling Li/O_2 cell, provided other parasitic reactions involving any of the implicated species do not occur concomitantly. Intriguingly, reaction 14 additionally implies a possible new battery chemistry in which NO_2 and O_2 are used

as oxidants in combination so that $LiNO_3$ is the discharge product. The specific energy of this system is 1748 Wh/kg based on the mass of $LiNO_3$ and the thermodynamically calculated cell voltage.

The process of persistent stabilization of the SEI on Li metal for rechargeable Li/O_2 batteries described in the present study can be summarized succinctly by a sum of reactions:

$$2Li + LiNO_3 \rightarrow LiNO_2 + Li_2O$$

$$LiNO_2 + \frac{1}{2}O_2 \rightarrow LiNO_3$$

$$2Li + \frac{1}{2}O_2 \rightarrow Li_2O$$
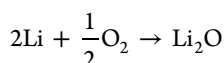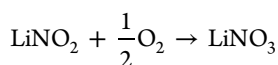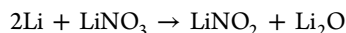
Previously, we suggested that the low solubility of O_2 in organic electrolytes prevents the formation of a compact enough SEI; However, O_2 has been observed to confer improvements in the Li metal SEI on its own in other solvents, although it is not sufficient to fully stabilize the SEI in DMA.

The use of NO_3^- in Li/O_2 cells creates new opportunities to engineer electrolyte compositions that may obviate the use of ceramic membrane materials to protect Li metal, which heretofore has shown poor performance in contact with O_2 electrodes containing organic solvents. The concepts outlined in this paper therefore represent a direction of research that may open new ways to practical realization of rechargeable Li/O_2 batteries.

■ ASSOCIATED CONTENT

Ⓢ Supporting Information

Description of the experimental methods, synthesis of lithium nitrite in nonaqueous solvent and its characterization, UV–visible data measurements, and methods of generating lithium nitrite and nitrate calibration curves in DMA. This material is available free of charge via the Internet at http://pubs.acs.org.

■ AUTHOR INFORMATION

Corresponding Author

*E-mail: jasim@liox.com, dan@liox.com.

Notes

The authors declare no competing financial interest.

■ ACKNOWLEDGMENTS

■ REFERENCES

(1) Bruce, P. G.; Freunberger, S. A.; Hardwick, L. J.; Tarascon, J.-M. Li-O_2 and Li-S Batteries with High Energy Storage. *Nat. Mater.* **2012**, *11*, 19−29.

(2) Christensen, J.; Albertus, P.; Sanchez-Carrera, S. R.; Lohmann, T.; Kozinsky, B.; Liedtke, R.; Ahmed, J.; Kojic, A. A Critical Review of Li/air Batteries. *J. Electrochem. Soc.* **2012**, *159*, R1−R30.

(3) Aurbach, D.; Zinigrad, E.; Cohen, Y.; Teller, H. A Short Review of Failure Mechanisms of Lithium Metal and Lithiated Graphite Anodes in Liquid Electrolyte Solutions. *Solid State Ionics* **2002**, *148*, 405−416.

(4) McCloskey, B. D.; Bethune, D. S.; Shelby, R. M.; Mori, T.; Scheffler, R.; Speidel, A.; Sherwood, M.; Luntz, A. C. Limitations in Rechargeability of Li-O_2 Batteries and Possible Origins. *J. Phys. Chem. Lett.* **2012**, *3*, 3043−3047.

(5) Freunberger, S. A.; Chen, Y. H.; Peng, Z.; Griffin, J. M.; Hardwick, L. J.; Barde, F.; Novak, P.; Bruce, P. G. Reactions in the

Rechargeable Lithium-O$_2$ Battery with Alkyl Carbonate Electrolytes. *J. Am. Chem. Soc.* **2011**, *133*, 8040−8047.

(6) Freunberger, S. A.; Chen, Y.-H.; Drewett, N. E.; Hardwick, L. J.; Barde, F.; Bruce, P. G. The Lithium-Oxygen Battery with Ether-Based Electrolytes. *Angew. Chem., Int. Ed.* **2011**, *50*, 8609−8613.

(7) Bryantsev, V. S.; Giordani, V.; Walker, W.; Blanco, M.; Zecevic, S.; Sasaki, K.; Uddin, J.; Addison, D.; Chase, G. V. Predicting Solvent Stability in Aprotic Electrolyte Li-Air Batteries: Nucleophilic Substitution by the Superoxide Anion radical (O$_2^{\bullet-}$). *J. Phys. Chem. A* **2011**, *115*, 12399−12409.

(8) Ryan, K. R.; Trahey, L.; Ingram, B. J.; Burrel, A. K. Limited Stability of Ether-Based Solvents in Lithium-Oxygen Batteries. *J. Phys. Chem. C* **2012**, *116*, 19724−19728.

(9) Walker, W.; Giordani, V.; Uddin, J.; Bryantsev, V. S.; Chase, G. V; Addison, D. A. Rechargeable Li-O$_2$ Battery Using a Lithium Nitrate/N, N-Dimethylacetamide Electrolyte. *J. Am. Chem. Soc.* **2013**, *135*, 2076−2079.

(10) Bryantsev, V. S.; Uddin, J.; Giordani, V.; Walker, W.; Addison, D.; Chase, G. V. The Identification of Stable Solvents for Nonaqueous Rechargeable Li-air Batteries. *J. Electrochem. Soc.* **2013**, *160*, A160−A171.

(11) Giordani, V.; Walker, W.; Bryantsev, V. S.; Uddin, J.; Chase, G. V.; Addison, D. Synergistic Effect of Oxygen and LiNO$_3$ on the Interfacial Stability of Lithium Metal in a Li/O$_2$ Battery. *J. Electrochem. Soc.* **2013**, *160*, A1544−A1550.

(12) Aurbach, D.; Pollak, E.; Elazari, R.; Salitra, G.; Kelley, C. S.; Affinito, J. On the Surface Chemical Aspects of Very High Energy Density, Rechargeable Li-Sulfur Batteries. *J. Electrochem. Soc.* **2009**, *156*, A694−A702.

(13) Liang, X.; Wen, Y. Z.; Liu, Y.; Wu, M. F.; Jin, J.; Zhang, H.; Wu, X. W. Improved Cycling Performances of Lithium Sulfur Batteries with LiNO$_3$-Modified Electrolyte. *J. Power Sources.* **2011**, *196*, 9839−9843.

(14) Pinicia, F.; Zambonin, P. G. Thermodynamics of the Systems NO$_3^-$ = NO$_2^-$ + 1/2 O$_2$ and NO$_3^-$ + 1/2 O$_2^{2-}$ = NO$_2^-$ + O$_2$- in Molten Alkali Nitrates. *J. Chem. Soc., Faraday Trans. 1* **1976**, *72*, 1512−1518.

(15) Boughriet, A.; Coumare, A.; Wartel, M. Electrochemical and Thermodynamic Behaviour of Oxygenated Nitrogen Compounds and Aromatic Hydrocarbons in Nitromethane, and the Nitration Processes with NO$_2^+$ (salvation phenomena). *Electrochim. Acta* **1990**, *35*, 389−397.

(16) Broder, T. L.; Silvester, D. S.; Aldous, L.; Hardacre, C.; Compton, R. G. Electrochemical Oxidation of Nitrite and the Oxidation and Reduction of NO$_2$ in the Room Temperature Ionic Liquids [C$_2$mim][NTf$_2$]. *J. Phys. Chem. B* **2007**, *111*, 7778−7785.

(17) Mishima, H.; Iwasita, T.; Macagno, V. A.; Giordano, M. C. The Electrochemical Oxidation of Nitrate ion on Platinum from Silver Nitrate in Acetonitrile Solutions-I. Kinetic Analysis. *Electrochim. Acta* **1973**, *18*, 287−292.

(18) Gary, R. M. *Synthetic Nitrogen Products: A Practical Guide to the Products and Processes*; Kluwer Academic/Plenum Publishers: New York, 2004.